

Green's function theory for infinite and semi-infinite particle chains

Y. Hadad* and Ben Z. Steinberg†

School of Electrical Engineering, Tel Aviv University, Ramat-Aviv, Tel-Aviv IL-69978, Israel

(Received 20 May 2011; revised manuscript received 11 August 2011; published 1 September 2011)

A Green's function theory for the excitation of, and scattering from, particle chains is developed. A Z transform is applied to the discrete dipole approximation of the chain, and the chain's spectral properties are explored in the complex Z plane. It is shown that a continuous spectrum may be excited, and the roles of the discrete and continuous spectra in the chain response are studied. The latter may dominate the chain response under lossy conditions. Using the Wiener-Hopf technique, the theory is extended to semi-infinite chains and the chain edge effects are studied. It is shown that edge effects can significantly enhance chain excitation.

DOI: 10.1103/PhysRevB.84.125402

PACS number(s): 78.67.Bf, 42.82.Et, 71.45.Gm, 42.25.Bs

I. INTRODUCTION

The electromagnetic properties of linear chains of identical and equally spaced microparticles have been studied in a number of previous publications.^{1–7} If the interparticle distance d is much smaller than the free-space wavelength λ , these structures can support the propagation of guided electromagnetic modes along the chain that does not radiate into the free space, with total width that can be much smaller than λ , hence, the name subdiffraction chains (SDC). If the particles are isotropic spheres, three independent electric dipole modes are supported; one with longitudinal e -dipole polarization p_z , and two degenerate modes with transverse and orthogonal polarizations p_x, p_y .⁷ Otherwise, more elaborate mode structures may exist.^{8–10} The interest in SDCs is motivated by both theoretical and practical points of view. Particle chains were proposed as guiding structures and junctions^{1–7} as a mechanism for coupling to surface waves⁸ and as polarization-sensitive waveguides.⁹ Very recently, it has been shown that magnetized spiral chains of plasmonic nanoellipsoids can be used as one-way optical waveguides.¹⁰ However, these previous studies essentially concentrated on the modal properties of the chain (i.e., a discrete set of guided and radiation waves), leaving out the continuous spectrum. A study of the SDC response to a general external excitation has not been addressed.

The purpose of this paper is to develop a rigorous Green's function theory that encapsulates all the wave phenomena associated with particle chains shown in Fig. 1, e.g., guided modes, radiation modes, and continuous spectrum. The Z transform^{11,12} (ZT) constitutes our basic mathematical tool. The resulting theory provides a framework for describing not only these spectral entities, but also a full-wave formulation for the response to external excitations of any kind. This may be of particular importance as the problem of chain excitation can not be addressed by using only the modes' dispersions; a procedure that determines the modes' weight, as well as the continuous spectrum weight, is needed. Furthermore, we employ a special Z transform extension of the Wiener-Hopf technique to solve rigorously the case of semi-infinite SDC (see examples in Refs. 13–15 for antenna arrays and for a two-dimensional wire or strips problems), a case of special importance as it incorporates edge effects that are inevitably excited in any realistic chain. These edge effects are given here explicit expressions describing the intermode couplings

and reflections occurring at the chain end, e.g., guided mode to guided mode, guided mode to light-line mode, etc. We note that particle chains of finite or semi-infinite length were studied so far only numerically,^{16–19} and the physical processes taking place at the edge remain unexplored. A careful comparison of our infinite and semi-infinite Green's functions is provided here and reconciled with the physical insight gained by the aforementioned edge coupling coefficients and with previous numerical studies done for particle chains of finite large length.^{16,17} We also show that the edge effect can significantly enhance chain excitation by external beams.

Why ZT and not conventional Fourier transform (FT)? Indeed, a formally exact representation of a particle-chain Green's function in terms of the FT has been derived and studied in, e.g., Refs. 16 and 17. In the FT approach, the Green's function is obtained by an inverse FT of its spectrum. Since the system under study is periodic with period d , this inverse FT is given by an integral that extends over the *finite* interval $\mathcal{R} = [-\pi/d, \pi/d]$: the reciprocal lattice domain. Hence, powerful tools of complex analysis based on closed-contour integration such as the residue theorem, Wiener-Hopf technique, etc., *can not* be invoked *unless* one rigorously maps \mathcal{R} to a closed-integration contour. This is precisely what the ZT is all about. The reciprocal lattice is mapped onto C_1 : the unit circle in the complex Z plane. The result is a powerful and physically transparent mathematical tool in which the Green's function wave constituents can be discerned directly from the *analytic properties* of the chain's spectra in the complex Z plane. Each singularity is a distinct wave phenomenon; poles moving on trajectories that follow C_1 represent guided modes, poles on trajectories directed inward or outward of C_1 are radiation modes, branch point and the associated branch cut constitute the continuous spectrum, etc. Their excitation strengths are nothing but the corresponding residues. Due to this analytical clarity, the aforementioned *new* wave phenomenon that was missed in previous studies based on the FT, i.e., the continuous spectrum wave, has been exposed. We show here that this wave can dominate the infinite or semi-infinite chain response and is practically not affected by material loss. This analytical clarity also sheds light on the somewhat artificial distinction made previously between "ordinary" and "extraordinary" waves^{16,17} (referred to, respectively as "guided" and "light-line" modes in Ref. 7), all of which are simple poles in the complex Z

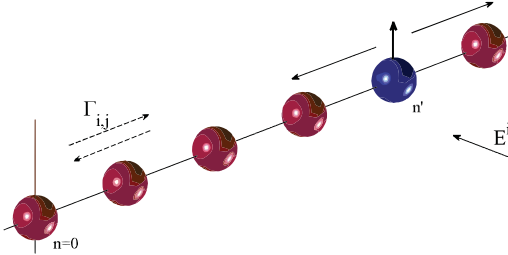


FIG. 1. (Color online) Excitation of (semi-) infinite particle chain.

plane, moving along various trajectories as the frequency is changed. Furthermore, we show that the “extraordinary” wave (“light-line” mode) *does not exist* in longitudinal polarization; the corresponding poles exist only in transverse polarization (consistent with Ref. 7). The continuous spectrum wave, due to a nearby branch point, is responsible for an excitation in the longitudinal polarization, which was misinterpreted as an “extraordinary” wave in Refs. 16 and 17.

Finally, it should be emphasized that a detailed analytical study of the infinite chain properties and singularities in the complex Z plane is carried out not only as a means to get a yet better understanding of the infinite chain physics. The infinite chain singularities tell us how to perform the analytic continuations that lie in the heart of the Wiener-Hopf technique and, as such, they play a crucial role for carrying out the semi-infinite case as well.

To obtain the equation governing the chain dynamics, we use the discrete dipole approximation (DDA) and polarizability theory.^{3–9} These hold when the particle diameter D is much smaller than the wavelength and the interparticle distance d is large compared to D . Studies show excellent agreement with exact solutions even when $d = 1.5D$.²⁰ Then, the ZT is applied to the governing equation and a spectral study is carried in the complex Z plane.

II. THEORY

Let α be the tensor polarizability of a reference particle in the structure shown in Fig. 1. All the particle properties (e.g., geometry, material, magnetization, etc.) are embedded in α .¹⁰ The chain dipole’s response \mathbf{p}_n ($n = 0, \pm 1, \pm 2, \dots$), due to an arbitrary incident field $\mathbf{E}^i(\mathbf{r})$, is governed by the matrix equation¹⁰

$$\alpha^{-1} \mathbf{p}_m - \epsilon_0^{-1} \sum_{n \neq m} \mathbf{A}[(m-n)d] \mathbf{p}_n = \mathbf{E}^i(\mathbf{r}_m). \quad (1)$$

Here, $\mathbf{r}_m = (0, 0, md)$ is the location of the m th particle, and $\mathbf{A}(z)$ is the free-space dyadic Green’s function, giving the free-space electric field at $\mathbf{r} = (0, 0, z)$ due to an infinitesimal dipole \mathbf{p} at $\mathbf{r}' = \mathbf{0}$:

$$\mathbf{E}(z) = \epsilon_0^{-1} \mathbf{A}(z) \mathbf{p}, \quad (2)$$

$$\mathbf{A}(z) = \frac{e^{ik|z|}}{4\pi|z|} \left[k^2 \mathbf{A}_1 + \left(\frac{1}{z^2} - \frac{ik}{|z|} \right) \mathbf{A}_2 \right] \quad (3)$$

with $\mathbf{A}_1 = \text{diag}(1, 1, 0)$, $\mathbf{A}_2 = \text{diag}(-1, -1, 2)$. We define the series of matrices \mathbf{D}_n :

$$\mathbf{D}_n = \begin{cases} -\epsilon_0^{-1} \mathbf{A}(nd), & n \neq 0 \\ \alpha^{-1}, & n = 0 \end{cases} \quad (4)$$

so Eq. (1) is rewritten as

$$\sum_n^{\infty} \mathbf{D}_{m-n} \mathbf{p}_n = \mathbf{E}_m^{i,r}, \quad \mathbf{E}_m^i \equiv \mathbf{E}^i(\mathbf{r}_m), \quad (5)$$

where the lower summation limit is $-\infty$ (0) for infinite (semi-infinite) chain, where in the former case it has a form of a discrete series convolution. The equation above can be analyzed and solved using the Z transform, a standard tool in spectral theory of difference equations¹¹ and discrete systems.¹² We apply the ZT to study the solution properties of our chains, using the (extended) double-sided ZT.¹² The ZT of a vector or matrix series is obtained by applying the conventional (scalar-series) ZT to each of the entries. Hence, the ZT of the series \mathbf{p}_n , denoted as $\bar{\mathbf{p}}$, is obtained by

$$\bar{\mathbf{p}}(Z) = \sum_{-\infty}^{\infty} \mathbf{p}_n Z^{-n} \quad (6)$$

and the transform of \mathbf{D}_n is obtained similarly. We assume that \mathbf{p}_n is bounded. Then, for $n \geq 0$ ($n < 0$), the series above is strictly convergent outside (inside) the circle $|Z| = R_+$ ($|Z| = R_-$, with $R_+ \leq 1 \leq R_-$) and is analytically continued to the complementary complex domain $|Z| \leq R_+$ ($|Z| \geq R_-$). Therefore, the series radius of convergence (ROC) is the ring $R_+ \leq |Z| \leq R_-$, which contains, in any case, the unit circle. The inverse ZT is given by

$$\mathbf{p}_n = \frac{1}{2\pi i} \oint_{C_{\pm}} \bar{\mathbf{p}}(Z) Z^{n-1} dZ. \quad (7)$$

The integration contour should lie on the ROC and encircle the origin in a counterclockwise direction. The unit circle (C_1) is an appropriate path; integration over it may be replaced by contributions of singularities. To that end, we define new paths C_{\pm} by $C_+ = C_1$ and $C_- = C_1 \cup C_{\infty}$. Here, C_{∞} encircles the complex Z plane at infinity in a clockwise direction. For the semi-infinite chain, the integration contour $C_{\pm} = C_+$ encircling all the singularities within the unit circle in the complex Z plane in a counterclockwise direction. For the infinite chain, the contour $C_{\pm} = C_+$ for $n \geq 0$, and $C_{\pm} = C_-$ for $n < 0$, encircling all the singularities *external* to the unit circle in the complex Z plane in a clockwise direction. In principle, the Z transform can be applied to Eq. (5) in order to solve rigorously for \mathbf{p}_n . For an infinite chain, Eq. (5) possesses a shift-invariant form (an infinite-series convolution) in which case it is transformed to a multiplication in the spectral (Z) plane. Then, the convolution operator is readily inverted. For a semi-infinite chain, the shift-invariance property is lost and we need a more elaborated tool to invert the semi-infinite difference operator. Below, we treat each of these cases separately.

A. Infinite chains

By applying the ZT to Eq. (5) with $-\infty$ as a lower bound and using the convolution theorem, one obtains, for $\bar{p}(Z)$,

$$\bar{p}(Z) = [\bar{\mathbf{D}}(Z)]^{-1} \bar{\mathbf{E}}^i(Z). \quad (8)$$

With the equation above, we define the chain's Green's function matrix series \mathbf{G}_n as the inverse ZT of $\bar{\mathbf{G}}(Z) = [\bar{\mathbf{D}}(Z)]^{-1}$:

$$\mathbf{G}_n = \frac{1}{2\pi i} \oint_{C_\pm} [\bar{\mathbf{D}}(Z)]^{-1} Z^{n-1} dZ. \quad (9)$$

This Green's function is the chain response due to an excitation of the $n = 0$ particle by a unit electric field vector. The response to an arbitrary excitation is obtained by the discrete convolution

$$\mathbf{p}_n = \sum_m \mathbf{G}_{n-m} \mathbf{E}_m^i \equiv \mathbf{G}_n * \mathbf{E}_n^i. \quad (10)$$

1. Analytic properties: Transverse excitation

The matrix $\mathbf{A}(nd)$ is diagonal. For transverse excitation, it is sufficient to consider only the first two entries. These two entries couple if the particle polarizability matrix α is nondiagonal, which takes place only for magnetized chains and/or when particle asymmetry is present.¹⁰ Here, we assume a simple chain made of nonmagnetized spherical particles with a scalar polarizability. Concentrating on the transverse excitation, we may consider only the first diagonal entry of each matrix in the matrix series \mathbf{D}_n , denoted now by the scalar series D_n . Applying the ZT, we have, for the infinite chain under transverse excitation,

$$\bar{D}(Z) = \frac{k^3}{4\pi\epsilon_0} \left[\frac{f_1(Z)}{kd} + \frac{if_2(Z)}{(kd)^2} - \frac{f_3(Z)}{(kd)^3} \right] - \frac{1}{\alpha}, \quad (11)$$

where we used $D_n = D_{-n}$. $f_s(Z)$ is defined as

$$f_s(Z) = Li_s(e^{ikd}Z) + Li_s(e^{-ikd}Z^{-1}), \quad (12)$$

and $Li_s(z)$ is the s th-order polylogarithm function²¹

$$Li_s(z) = \sum_{n=1}^{\infty} \frac{z^n}{n^s} \Rightarrow Li'_s(z) = z^{-1} Li_{s-1}(z), \quad (13)$$

with $Li_0(z) = z/(1-z)$, $Li_1(z) = -\ln(1-z)$. Additional properties of the polylogarithm functions needed here are presented in Appendix A. Generally, $Li_s(z)$ inherits the singularity of $\ln(1-z)$ $\forall s \geq 1$, possessing Riemann sheets of infinite multiplicity. In the zeroth Riemann sheet (R0), $f_s(Z)$ possesses two branch points $Z_{b1,2}$ and two branch cuts

$$Z_{b1,2} e^{\pm ikd} = 1. \quad (14)$$

One cut emerges from the branch point at $Z_{b1} = e^{-ikd}$ and extends to infinity, and a second cut emerges from a branch point at $Z_{b2} = e^{ikd}$ and extends to the origin. $\bar{D}(Z)$ and the Green's function spectrum $\bar{\mathbf{G}}(Z)$ possess exactly the same branch singularities. These branches constitute the chain continuous spectrum, which has not been studied before. These branch points result solely from the analytic properties of the polylogarithm functions (which in turn result from interparticle interactions). Hence, they are *independent of the*

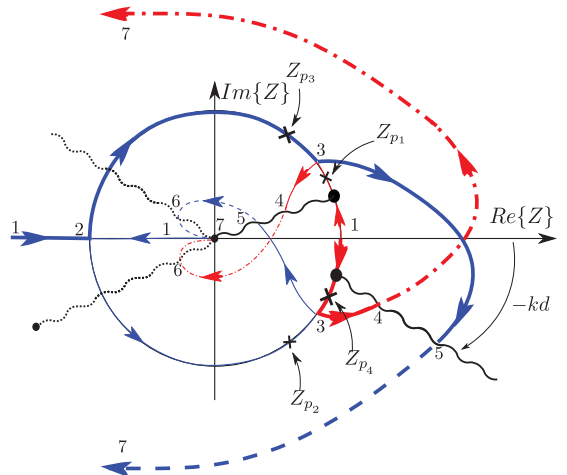


FIG. 2. (Color online) The analytic properties of the spectral Green's function $\bar{\mathbf{G}}(Z)$ in the complex Z plane for transverse excitation. The poles, shown by \times , convey the chain modes' excitation. The branch cuts, shown by wiggly lines, convey the continuous spectrum excitation.

particle material. This fact is of importance for understanding the complete chain behavior in the presence of loss. In addition, $\bar{\mathbf{G}}(Z)$ possesses poles $Z_p(\omega)$ in the complex Z plane, given by the zeros of $\bar{D}(Z)$ in Eq. (11). These poles represent the chain modes reported in previous publications (see Refs. 3–5 for theoretical analysis, Ref. 6 for interesting experimental verifications, and Ref. 7 for a comprehensive exposition). Since the zeros of Eq. (11) depend on α , pole locations may depend on material and are influenced by loss. The previously derived modes' dispersion relations $\beta(\omega)$ are obtained from $Z_p(\omega)$ by

$$e^{i\beta d} = Z_p(\omega). \quad (15)$$

From the symmetry of f_s with respect to Z , it follows that, if $Z_{p\ell}$ is a pole, then $Z_{p\ell'} = Z_{p\ell}^{-1}$ is also a pole; the number of poles is always even. Clearly, for lossless particles, the chain-propagating modes are obtained by poles located exactly on the unit circle: $|Z_p| = 1$. The chain-radiation modes are obtained by poles inside the unit circle for $n \geq 0$, and by poles outside the unit circle for $n < 0$. We have computed numerically the pole locations for an infinite chain of lossless plasmonic spherical inclusions (typical pole dynamics is shown in Fig. 2).

Referring to the figure, branch points are shown by solid black circles, branch cuts by wiggly lines, and poles are marked by black \times , all for a specific frequency. Pole trajectories as a function of frequency are denoted by solid color lines in the zeroth Riemann sheet R0, by dashed-dotted lines in the -1 Riemann sheet (R-1), and by dashed line in R1 (dotted wiggly lines correspond to branch cuts in R1 and R-1.) The evolution of the branch points as a function of frequency is omitted to avoid cluttering the figure. As pointed out before, there are four poles. We denote by $Z_{p1,2}$ ($Z_{p3,4}$) the poles pertaining to propagation in $n > 0$ ($n \leq 0$). At very low frequencies, two poles $Z_{p1,4}, Z_{p4} = Z_{p1}^{-1}$ are located in R0 on the unit circle near $Z = 1$ at location #1, just above the upper branch point at e^{ikd} and below the lower branch point at e^{-ikd} . Their location indicates that they correspond to

propagation modes of the chain, with characteristic dispersion very close to the light line (denoted light-line modes in Ref. 7, or extraordinary waves in Ref. 16). They possess no low-frequency cutoff, and their evolution with frequency is shown by the red (continuous line, that is followed by dashed-dotted) lines. For $\omega < \omega_3$, their location remains close to the branch points (the latter evolve along the unit circle). Note that, at the branch singularities (14), we have $\lim_{Z \rightarrow Z_{b,1,2}} \tilde{G}(Z) = 0$; hence, whenever $Z_{p,1,4}$ are close to $Z_{b,1,2}$, the corresponding residues are very small, thus establishing mathematically the observation made heuristically in Ref. 7 that the “light-line modes” excitation and interaction with the chain are very weak.

Two additional poles $Z_{p,2,3}, Z_{p,3} = Z_{p,2}^{-1}$ emerge from the origin and from $Z = -\infty$ in R0 and move along the blue trajectories toward $Z = -1$. They reach point #2 at frequency ω_2 , representing the lower cutoff of the corresponding chain-propagating modes. When these poles move along the unit circle, the corresponding waves possess real wave number larger than k and they constitute modes that propagate along the chain with no radiation to the free space. These modes are termed as “guided modes” in Ref. 7, and “ordinary waves” or “quasistatic waves” in Ref. 16. As frequency increases, all these four poles evolve along the unit circle toward point #3. The corresponding frequency ω_3 is the upper cutoff of the chain modes. For $\omega > \omega_3$, the poles represent radiation modes, which move along the continuous red and blue trajectories and intersect the branch cuts at points #4 and #5 at frequencies $\omega_{4,5}$, respectively, residing thereafter in the R-1 (dashed-dotted red line) and R1 (dashed blue line). It should be emphasized that, for $\omega > \omega_5$, the chain Green’s function consists of branch cut (i.e., continuous spectrum) contribution only; in this frequency domain, no propagation modes or radiation modes are supported by the chain.

Finally, note that, when losses are present, $Z_{p,1,2}$ ($Z_{p,3,4}$) are slightly shifted inward (outward) of the unit circle, but the branch point locations are not affected.

An expression for G_n can be obtained by using Eq. (11) in the inverse ZT (9), exploiting the analytic properties discussed above. We have

$$G_n = \sum_m G_n^{(p_m)} + G_n^{(b)}, \quad (16)$$

where $G_n^{(p_m)}$ and $G_n^{(b)}$ are the m th pole and the branch-cut contributions to the Green’s function, representing the discrete and continuous spectra, respectively. They are given by

$$G_n^{(p_m)} = \text{sgn}(n) \frac{1}{\bar{D}'(Z_{p_m})} Z_{p_m}^{n-1}, \quad (17)$$

$$G_n^{(b)} = \frac{1}{2\pi i} \int_{C_b} \frac{1}{\bar{D}(Z)} Z^{n-1}. \quad (18)$$

In the above, $\text{sgn}(x) = 1$ for $x \geq 0$ and -1 elsewhere. Z_{p_m} is the m th pole located inside (outside) the unit circle, C_b is an integration path that encircles the branch cut inside (outside) the unit circle in a counterclockwise (clockwise) direction for $n \geq 0$ ($n < 0$). By using Eqs. (11)–(13), one can express \bar{D}' in terms of Lis , and simplify Eq. (17). By defining

$$g_s(Z) = Lis(e^{ikd}Z) - Lis(e^{ikd}Z^{-1}), \quad (19)$$

$G_n^{(p_m)}$ can be written explicitly as

$$G_n^{(p_m)} = \frac{\text{sgn}(n) 4\pi \epsilon_0 d / k^2}{\sum_{s=0}^2 \left(\frac{i}{kd}\right)^s g_s(Z_{p_m})} Z_{p_m}^n. \quad (20)$$

The characteristic behavior of $Z_{p_m}^n$ is nothing but the propagation of a guided or radiation mode in the structure [see Eq. (15)]. Note that, for $n \geq 0$ ($n < 0$), only the poles inside (outside) the unit circle are included.

A similar expression for the continuous spectrum wave in Eq. (18) is not available. However, the branch-cut integral can be evaluated asymptotically for large $|n|$ (see Appendix B). It yields the interesting wave-type result

$$G_n^{(b)} \simeq \frac{4\pi \epsilon_0 d}{k^2} \frac{e^{i|n|kd}}{|n|} \prod_{m=1}^2 \frac{1}{\ln |n| + A_m}, \quad |n| \gg 1 \quad (21)$$

where the coefficients A_m are given in Appendix B. Evidently, this wave radiates to the free space as it propagates along the chain and decays in a rate that is inversely proportional to $n(\ln n)^2$. It oscillates with a spatial period of the vacuum wavelength. Note that the particle material enters only via the algebraic dependence of $A_{1,2}$. Therefore, *material loss does not result in exponential decay*; its effect is limited to an algebraic change of the wave amplitude.

The various waves of G_n in a chain of plasmonic spheres were calculated with the following parameters. The inter-particle distance d and particle radius a are $d = \lambda_p/30$, where λ_p is the plasma frequency wavelength, and $a = 0.25d$, respectively. Several excitation frequencies were examined. Figure 3 shows the various waves at $\omega/\omega_p = 0.580907$, satisfying $\omega_2 < \omega < \omega_3$. Formally, two poles on the unit circle (guided and light-line modes) and branch-cut spectra are excited. However, the light-line mode is extremely weak, and the continuous spectrum is significant only near the source. The asymptotic expression for the continuous spectrum is shown in the inset by a black dashed line. It matches by amplitude and phase, but, for clarity, only the envelope is shown. Figure 4

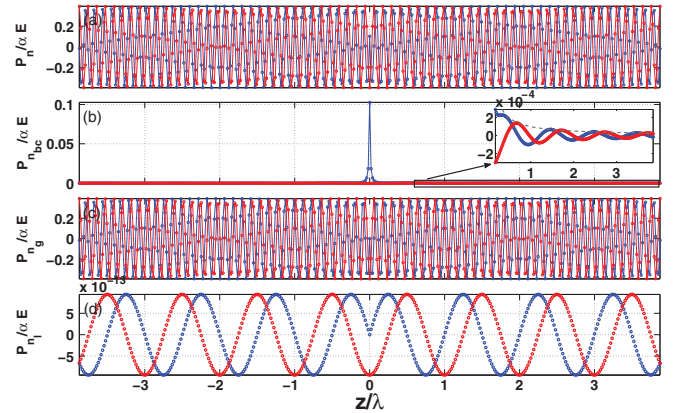


FIG. 3. (Color online) G_n for transverse excitation and its wave contributors at $\omega/\omega_p = 0.580907$ ($\omega_2 < \omega < \omega_3$). Real and imaginary parts are shown by blue and red lines, respectively. (a) G_n . (b) The continuous spectrum wave. The envelope of Eq. (21) is shown in the inset by black dashed line. (c) The guided mode. (d) The light-line mode. Note that its excitation is $O(10^{-12})$ weaker compared to the other waves.

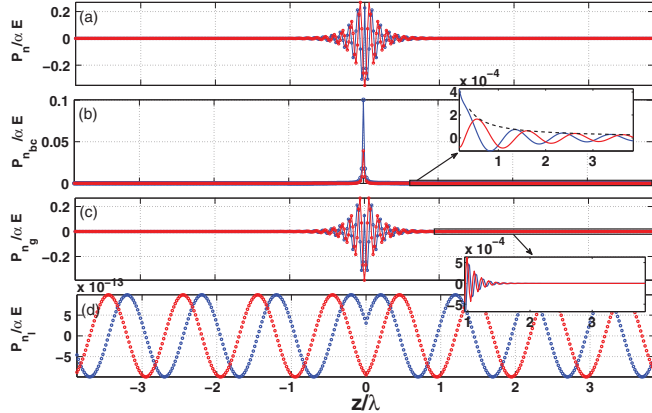


FIG. 4. (Color online) The same as Fig. 3, but for gold particles with losses $1/\tau = 0.0023\omega_p$. The continuous spectra dominate at large distances. Again, note that its excitation is $O(10^{-12})$ weaker compared to the other waves.

is the same as Fig. 3, but with losses of gold particles. The continuous spectrum dominates at large distance.

The second frequency is $\omega/\omega_p = 0.587\,677$, satisfying $\omega_4 < \omega < \omega_5$. The light-line poles are in R-1 and do not contribute. The poles $Z_{p,2,3}$ are still on R0, inside and outside the unit circle, corresponding to radiation modes at $n \geq 1$ and $n < 0$, respectively. The pole and branch-cut contributions are plotted in Fig. 5. The latter are comparable to the former.

2. Analytic properties: Longitudinal excitation

Here, we may consider only the third diagonal entry in \mathbf{D}_n , generating a different scalar series D_n . Applying the ZT, we obtain

$$\bar{D}(Z) = \frac{k^3}{2\pi\epsilon_0} \left[-\frac{if_2(Z)}{(kd)^2} + \frac{f_3(Z)}{(kd)^3} \right] - \frac{1}{\alpha}. \quad (22)$$

Hence, the branch point and branch cut of $\mathbf{G}(Z)$ are identical to those of the transverse excitation, but we have only two poles [zeros of Eq. (22)]. The properties are shown in Fig. 6.

The light-line poles, which exist under transverse excitation and possess no low-frequency cutoff (shown by red trajectories

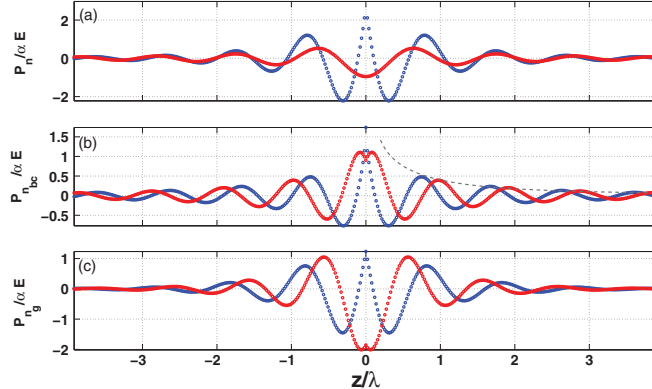


FIG. 5. (Color online) The same as Fig. 3, but for $\omega/\omega_p = 0.587\,677$ ($\omega_4 < \omega < \omega_5$). (a) G_n . (b) The continuous spectrum wave. The envelope of Eq. (21) is shown by a black dashed line. (c) The radiation mode (guided mode pole above its cutoff at ω_4 .)

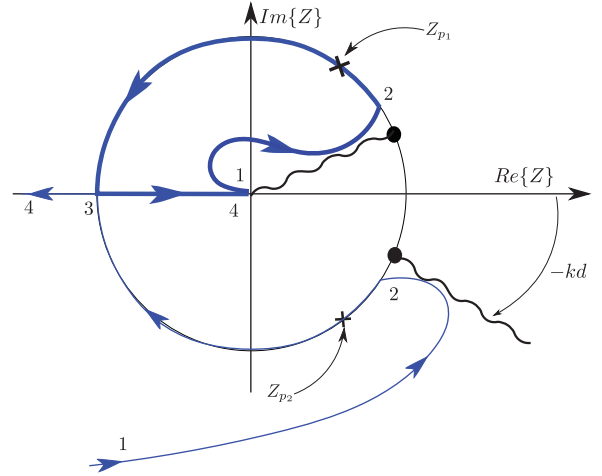


FIG. 6. (Color online) The analytic properties of $\bar{G}(Z)$ in the complex Z plane for longitudinal excitation.

in Fig. 2), are not present. This is consistent with Ref. 7. The poles emerge from $Z \rightarrow \infty$ at the third quadrant and $Z = 0$ at very low frequency, and move toward point #2 as the frequency increases. They reach point #2 at frequency ω_2 corresponding to the lower cutoff of the propagation band. As the frequency increases, the poles move along the unit circle toward point #3, reaching it at frequency ω_3 corresponding to the upper cutoff of the propagation modes. For $\omega > \omega_3$, the poles move along the negative real axis toward $Z = 0, -\infty$, becoming again radiation modes.

B. Semi-infinite chains

In the case of semi-infinite chains, Eq. (5) still holds, but with lower summation bound $n = 0$ and equation index $m \geq 0$. Since the shift-invariance property is lost, the convolution theorem can not be directly applied. A special extension of the Weiner-Hopf technique, presented in Refs. 13,14 for different applications, may be used to solve this difficulty. We apply this approach and put special emphasis on the wave interpretation of the various spectral contributors. Following Ref. 13, we define the + and - series as pertaining, respectively, to $n \geq 0$ and $n < 0$ for all quantities involved. Hence,

$$x_n^+ = \begin{cases} x_n, & n \geq 0 \\ 0, & n < 0 \end{cases}, \quad x_n^- = \begin{cases} 0, & n \geq 0 \\ x_n, & n < 0 \end{cases} \quad (23)$$

where x_n stands for p_n, E_n , etc. From Eq. (6), the ZT of the + (-) series are analytic in $|Z| \geq 1$ ($|Z| < 1$), a property that plays a pivotal role in subsequent analysis. Equation (5) can be rewritten as (we omit the “ i ”)

$$\sum_{m=-\infty}^{\infty} D_{m-n} p_n^+ = E_m^+ + E_m^-, \quad \forall m. \quad (24)$$

In the *actual* chain, p_n, E_n are not defined for $n < 0$. Hence, p_n^-, E_n^- do not have any physical role; they are used only as entities that enable the extension of Eq. (5) to the shift-invariant form in Eq. (24). However, the series D_n is defined for all n and is identical to that of the infinite chain; its ZT is still given by Eq. (11), with the same ROC. Note that we are not looking for the Green's function of the equation above; it was derived

in the previous section. Rather, we look for the solution of Eq. (24) for the right-hand side with $E_n^+ = \delta_{n-n'} +$ the implied E_m^- [such that Eq. (23) is satisfied]. This is the Green's function $G_{n,n'}$ of the semi-infinite chain. The response to any incident field E_n^i is then

$$p_n = p_{n|n \geq 0}^+ = \sum_{n'=0}^{\infty} G_{n,n'} E_{n'}^i. \quad (25)$$

We apply the ZT to Eq. (24), and decompose $\bar{D}(Z)$ as

$$\bar{D}(Z) = D^+(Z)D^-(Z), \quad (26)$$

where $D^+(Z)$ [$D^-(Z)$] is analytic in $|Z| \geq 1$ ($|Z| < 1$), with no zeros there. Due to this analyticity, and since $\bar{D}(Z) = \bar{D}(Z^{-1})$, we have

$$D^+(Z) = D^-(Z^{-1}). \quad (27)$$

Explicit expressions for $D^+(Z)$ in terms of $\bar{D}(Z)$ can be derived (see Appendix C). Its value in $|Z| > 1$ and its analytic continuation into the unit circle are given by

$$D^+(Z) = \frac{1}{\lambda_0} \exp \frac{1}{2\pi i} \oint_{C_1} \frac{\ln \bar{D}(\zeta)}{Z - \zeta} d\zeta, \quad |Z| > 1 \quad (28)$$

$$D^+(Z) = \frac{\bar{D}(Z)}{\lambda_0} \exp \frac{1}{2\pi i} \oint_{C_1} \frac{\ln \bar{D}(\zeta)}{Z - \zeta} d\zeta, \quad |Z| \leq 1. \quad (29)$$

$D^-(Z)$ is obtained via Eq. (27). λ_0 is given by

$$\lambda_0 = \exp \frac{-1}{4\pi i} \oint_{C_1} \frac{\ln \bar{D}(\zeta)}{\zeta} d\zeta \quad (30)$$

and we have

$$D^-(0) = \lim_{Z \rightarrow \infty} D^+(Z) = \lambda_0^{-1}. \quad (31)$$

Application of the ZT on Eq. (24) now yields

$$D^+(Z)\bar{p}^+(Z) = \frac{\bar{E}^+(Z)}{D^-(Z)} + \frac{\bar{E}^-(Z)}{D^-(Z)}. \quad (32)$$

The second term on the right-hand side above is analytic inside the unit circle. The first term can be decomposed as

$$\frac{\bar{E}^+(Z)}{D^-(Z)} = \left(\frac{\bar{E}^+}{D^-} \right)^+(Z) + \left(\frac{\bar{E}^+}{D^-} \right)^-(Z) \quad (33)$$

with which Eq. (32) can be rewritten as

$$D^+(Z)\bar{p}^+(Z) - \left(\frac{\bar{E}^+}{D^-} \right)^+(Z) = \left(\frac{\bar{E}^+}{D^-} \right)^-(Z) + \frac{\bar{E}^-(Z)}{D^-(Z)}. \quad (34)$$

The two sides of the equality above are analytic on *complementary domains* in the complex Z plane with common region of analyticity on $|Z| = 1$. Thus, by analytic continuation, we may define an *entire* function. Let us denote this function by $\Pi(Z)$. In addition, in view of Eq. (31) and of $\lim_{Z \rightarrow \infty} \bar{p}^+(Z) = p_0^+$ [see Eq. (6)], we must have $\lim_{Z \rightarrow \infty} D^+\bar{p}^+ = p_0^+/\lambda_0 = \text{const}$. Also, by considering the analytic properties of D^- outside the unit disk, it may be shown that $\lim_{Z \rightarrow \infty} (\bar{E}^+/D^-)^+ = \text{const}$. Furthermore, there is an additive constant flexibility in the “+” and “-” decomposition in Eq. (33). We choose this additive constant such that $\lim_{Z \rightarrow \infty} (\bar{E}^+/D^-)^+ = p_0^+/\lambda_0$, so at $Z \rightarrow \infty$, the left-hand side of Eq. (34) vanishes, i.e.,

$\lim_{Z \rightarrow \infty} \Pi(Z) = 0$, yielding that $\Pi(Z)$ is bounded. Finally, we apply Liouville theorem (every bounded entire function must be a constant) on $\Pi(Z)$, concluding that $\Pi(Z) \equiv 0$. This yields that $\forall Z$ the left- and the right-hand sides in Eq. (34) vanish. Hence, the left side implies

$$\bar{p}^+(Z) = \left(\frac{\bar{E}^+}{D^-} \right)^+(Z) \frac{1}{D^+(Z)}. \quad (35)$$

Since $(\bar{E}^+/D^-)^+$ is analytic outside the unit circle, it may be expanded by a Laurent series

$$\left(\frac{\bar{E}^+}{D^-} \right)^+(Z) = \sum_{j=0}^{\infty} a_j Z^{-j}, \quad (36)$$

where the coefficients a_j may be obtained directly from a generalization of Cauchy's integral formula. We are mainly interested in the chain Green's function: the response to the excitation $E_n^i = \delta_{n-n'} (n' \geq 0)$. Hence, $\bar{E}^+(Z) = Z^{-n'}$. Then (see Appendix D),

$$a_j = \begin{cases} \frac{1}{2\pi i} \oint_{C_1} \frac{Z^{j-n'-1}}{D^-(Z)} dZ, & j \leq n' \\ 0, & j \geq n'+1. \end{cases} \quad (37)$$

We now apply inverse ZT to Eq. (35), use Eqs. (36) and (37), and substitute D^+ via Eq. (27) with a change of variable. The result for the semi-infinite chain Green's function (p_n for $\delta_{n-n'}$ excitation) is

$$G_{n,n'} = \sum_{j=0}^{\infty} \lambda_{n'-j} \lambda_{n-j}, \quad (38)$$

where

$$\lambda_s = \begin{cases} \frac{1}{2\pi i} \oint_{C_1} \frac{Z^{s-1}}{D^+(Z)} dZ, & s \geq 0 \\ 0, & s < 0 \end{cases} \quad (39)$$

which reduces to λ_0 in Eqs. (30) and (31) for $s = 0$ (use analyticity of D^+ and Cauchy theorem).

1. Wave content and physical interpretation

While Eqs. (38) and (39) are formally complete and exact, the wave content of the semi-infinite chain excitation remains obscured. Below, we use the properties of D^+ *inside* the unit circle via Eq. (29) in order to rewrite the result in terms of the *cogent* wave components excited in the chain, and their interaction with the chain end. First, note that the exponent in Eq. (29) is analytic and does not vanish for any $|Z| \leq 1$. Hence, $1/D^+$ and $1/\bar{D}$ have exactly the same singularities inside the unit circle: two poles and one branch cut (see discussion in Sec. II A.) Therefore, Eq. (39) can be replaced by two pole residues and one branch-cut integration

$$\lambda_n = \sum_{m=1}^2 \kappa_m G_n^{(p_m)} + \frac{1}{2\pi i} \oint_{C_b} \frac{Z^{n-1}}{D^+(Z)} dZ, \quad (40)$$

where we have used Eqs. (17), (19), and (20), and the coefficient κ_m is given by

$$\kappa_m = \lambda_0 \exp \frac{-1}{2\pi i} \oint_{C_1} \frac{\ln \bar{D}(\zeta)}{Z_{p_m} - \zeta} d\zeta. \quad (41)$$

Note that $G_n^{(p_m)}$ is nothing but the pole (mode) excitation in the infinite chain. Substituting this into Eq. (38) and rearranging, we obtain the following *physically meaningful* expression:

$$G_{n,n'} = \sum_{m=1}^2 G_{|n-n'|}^{(p_m)} + G_{|n-n'|}^{(b)} \quad (42)$$

$$+ \sum_{m,m'=1}^2 G_n^{(p_m)} G_{n'}^{(p_{m'})} \Gamma_{m,m'} \quad (43)$$

$$+ \sum_{m=1}^2 [G_{n'}^{(p_m)} B_n^{(m)} + G_n^{(p_m)} B_{n'}^{(m)}] \quad (44)$$

$$+ b_{n,n'}. \quad (45)$$

Clearly, the first three terms summed in Eq. (42) represent free chain modes and continuous spectrum, propagating from particle n' to particle n . The terms summed in Eq. (43) represent chain modes m' excited at n' , which propagate to the chain end, get converted to mode m , and then reflected back to the observer at n . The coupling and reflection coefficient $\Gamma_{m,m'}$ describing this process is given by

$$\Gamma_{m,m'} = \kappa_m \kappa_{m'} \frac{Z_{p_m} Z_{p_{m'}}}{Z_{p_m} Z_{p_{m'}} - 1}. \quad (46)$$

The first summed terms in Eq. (44) represent chain modes (excited at n') that hit the chain end, get converted to continuous spectrum, then propagate back to the observer at n . The conversion from mode m to continuous spectrum and the propagation thereof are given by $B_n^{(m)}$:

$$B_n^{(m)} = \frac{\kappa_m}{2\pi i} \int_{C_b} \frac{Z^{n-1}}{D^+(Z)} \frac{ZZ_{p_m}}{ZZ_{p_m} - 1} dZ. \quad (47)$$

The second summed terms in Eq. (44) represent the continuous spectrum (excited at n') that hits the chain end and gets converted to a chain mode (m) that propagates to the observer at n . $B_{n'}^{(m)}$ is given by Eq. (47) with $n \rightarrow n'$. Finally, $b_{n,n'}$ represents the continuous spectrum that hits the chain end and gets reflected as continuous spectrum. It is given by

$$b_{n,n'} = \frac{-1}{4\pi^2} \int_{C_b} \frac{ZZ'}{ZZ' - 1} \frac{Z^{n-1} Z'^{n'-1}}{D^+(Z) D^+(Z')} dZ dZ'. \quad (48)$$

In Fig. 7, the magnitude and phase of $\Gamma_{mm'}$ are shown as a function of frequency for a chain with the same parameters as the one discussed in the example concluding Sec. II A 1. It is seen that conversion from *any* mode into a light-line mode at the chain end is practically zero. Both modes, light line (pole #1) and guided (pole #2), are converted mostly into a reflected guided mode. This can explain how edge effects enhance chain excitation.

2. Example for the effect of the edge on G

There are previously reported studies on finite-length particle chains and edge effects (see, e.g., Refs. 16–19). All are essentially based on numerical simulation. In Ref. 16, however, effort is made to base the study of finite- (but long) chain Green's function on that of the infinite chain. Since in such an approach a deep understanding of the infinite chain case is crucial, and since our analysis in Sec. II B 1 is targeted at

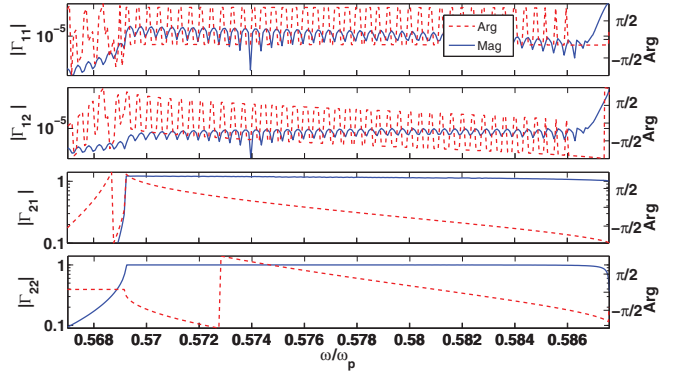


FIG. 7. (Color online) $\Gamma_{i,j}$ vs ω . Γ_{11} = light line to light line; Γ_{12} = guided to light line; Γ_{21} = light line to guided; Γ_{22} = guided to guided.

this very same goal, we turn to discuss our analysis in light of the examples simulated in Ref. 16. Thus, we consider a chain with parameters identical to those of Ref. 16: $\omega = \omega_p/\sqrt{3}$, $d = \lambda/10$, $a = d/4$, $1/\tau = 0.002\omega_p/\sqrt{3}$. We computed $G_{n,n'}$ for infinite and for the semi-infinite chains, both with $n' = 0$. The results are compared in Fig. 8. Few observations can be made. In the domain near the source (for these specific parameters, $n - n' \lesssim 50$), the curves are practically identical. That is, G for infinite and semi-infinite chains differs only by a constant multiplication factor, given in this example by $G_{0,0}^{\text{inf}}/G_{0,0}^{\text{semi-inf}} \approx -1.61+i0.08$. However, the two solutions deviate for larger distances. Hence, the statement made in Ref. 16 that the Green's function of infinite and semi-infinite chains differs only by a multiplication factor is somewhat incomplete; it is correct only within the limited region near the source. The physics behind this fact is explained as follows. First, recall our results of Sec. II A 1. In the infinite chain, the dominant wave constituent is the guided mode: pole #2 has the largest residue. The excitation strengths of the light-line mode and the continuous spectrum wave (pole #1 and branch cut) are of the same order, and both are orders of magnitude smaller compared to pole #2. The passage to semi-infinite chain can be achieved by summing these wave constituents weighted by their corresponding reflection and coupling coefficients in Eqs. (42)–(48). Due to the dominance of pole #2, it is mainly given by Γ_{22} , which is close to unity (see Fig. 7). However,

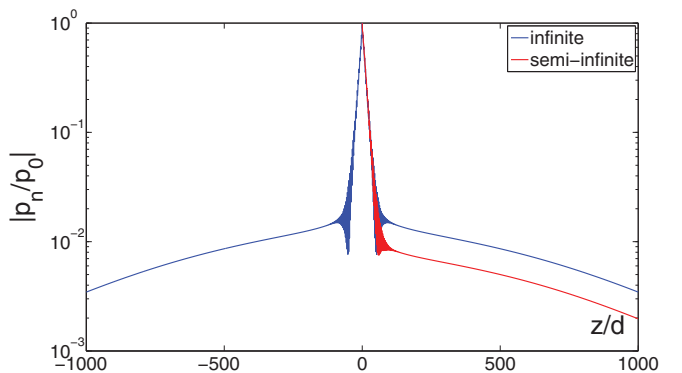


FIG. 8. (Color online) The transverse excitation $G_{n,0}$ for infinite and semi-infinite chains, normalized to their maximum value (at the source location $n = n' = 0$).

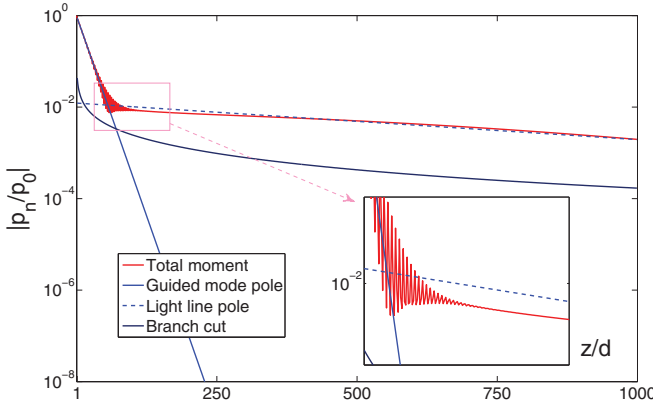


FIG. 9. (Color online) The transverse excitation $G_{n,0}$ for semi-infinite chains, decomposed into its various components. Chain parameters are the same as for Fig. 8 and Fig. 2 of Ref. 16.

loss is present so this wave decays exponentially. Then, since the *continuous spectrum wave is not affected by loss*, and the light-line pole decay is slower than that of the guided mode, they take over after a short distance, and both possess different reflection coefficients. The fact that the lines in Fig. 8 for large $|n - n'|$ are curved and not straight confirms that the continuous spectrum has an important contribution {note the $1/[n \ln^2(n)]$ behavior in Eq. (21) and the logarithmic scale in the figure}.

To make a final assessment of these observations, $G_{n,0}$ of the semi-infinite chain is decomposed into its various components. They are shown in Fig. 9. Chain parameters are identical to those of Fig. 8 and Fig. 2 of Ref. 16. It is seen that the light-line wave and the continuous spectrum wave are much weaker than the excitation of the guided mode *near the source*. Away from the source, the continuous spectrum wave can not be neglected. Furthermore, away from the source, the light-line mode (pole #1) has an exponential decay, while the continuous spectrum wave decays slower than an exponential. Finally, Fig. 10 shows the components of $G_{n,0}$ for a semi-infinite chain with the same parameters as in Fig. 4(a) of Ref. 16: $\omega = 0.984\omega_p/\sqrt{3}$, $1/\tau = 0.002\omega_p/\sqrt{3}$. With these parameters, one pole in R0 (principal Riemann sheet) is located deep inside the unit circle in the Z plane (blue line in Fig. 2 between

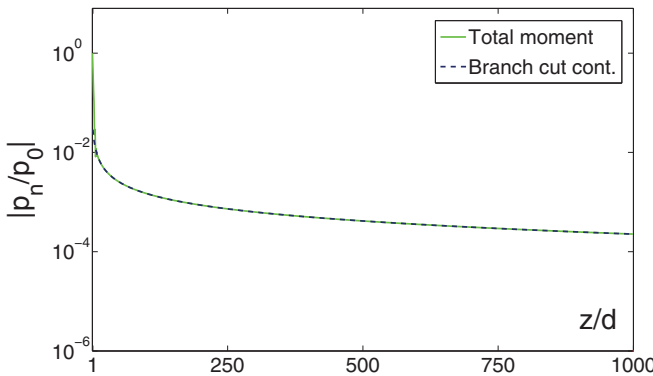


FIG. 10. (Color online) The transverse excitation $G_{n,0}$ for semi-infinite chains, decomposed into its various components. Chain parameters are the same as for Fig. 4(a) of Ref. 16.

points #1 and #2), thus, the corresponding wave decays very fast. The second pole, corresponding to the light-line mode, is very close (lossy) or on (lossless) the unit circle. However, due to its proximity to the branch point, its residue is $O(10^{-5})$ smaller than the other wave constituents, so its excitation is completely negligible (see discussion in Sec. II A 1 regarding the residue of the light line pole, and Figs. 3 and 4). Hence, the only contributing wave is the continuous spectrum [and not the light-line (extraordinary) wave as stated in Ref. 16]. Actually, the fact that the solution does not appear as a straight line in a logarithmic scale indicates that this wave decays algebraically [see Eq. (21)] and not exponentially, so it can not be a simple pole.

III. EXCITATION BY A BEAM

We examine the excitation of a chain by a \hat{x} -polarized Gaussian beam (GB) hitting the chain at its waist. The beam axis crosses the chain at particle n_c , and is tilted at angle ϑ relative to the chain axis. The incident field at the n th particle is

$$E_n^i = \sqrt{\frac{w_0}{w_n}} e^{ik[\bar{n}d \cos \vartheta + \frac{(\bar{n}d \sin \vartheta)^2}{2w_n}]} \quad (49)$$

with $w_n = \bar{n}d - iF$ and $\bar{n} = n - n_c$. F is the beam collimation distance, chosen as $F = 500d$. The beam frequency is chosen to be inside the chain propagation band $\omega/\omega_p = 0.580\,907$, yielding zeros of Eq. (11) at $Z_{p1} = e^{i0.12166}$, $Z_{p2} = e^{-i1.05225}$, and at the conjugate locations. Two cases are considered: a semi-infinite chain with the GB hitting the chain at its end, and excitation of an infinite chain; for both, $n_c = 0$. We calculate the Green's function via Eq. (16) [Eq. (38)] and use the convolution in Eq. (10) [superposition in Eq. (25)] with the excitation series Eq. (49), for infinite (semi-infinite) chain. The numerical results are shown in Fig. 11. Figures 11(a) and 11(b) show the incident field E_n^i for semi-infinite and infinite chains, respectively. Figures 11(c) and 11(d) show the chain response. It is seen that when the beam hits the chain end [Fig. 11(c)], the chain-propagating mode is strongly excited, and the chain response is very noticeable also away from the lit region. However, when the incident field does not interact with the chain end [Fig. 11(d)], the chain-propagating mode is practically not excited and the chain response in regions remote from the lit domain is practically zero. The reason for the significant excitation enhancement by the edge is as follows. The beam is a free-space wave and, as such, it is orthogonal to the guided modes of reciprocal waveguides.²² Since its spatial variation scale is approximately the vacuum wavelength, it couples only to the light-line mode (which possesses the same length scale), but this coupling is very weak in infinite chains due to the small residue (see Sec. II A 1). However, for semi-infinite chains, this orthogonality is lost, and further, since $|\Gamma_{21}|, |\Gamma_{22}| \approx 1$ (see Fig. 7), the edge converts both modes to a reflected guided mode.

IV. CONCLUSION

A rigorous Green's function theory has been developed for infinite and semi-infinite particle chains. The theory uses the Z transform (ZT) as its basic spectral tool. In this theory, the

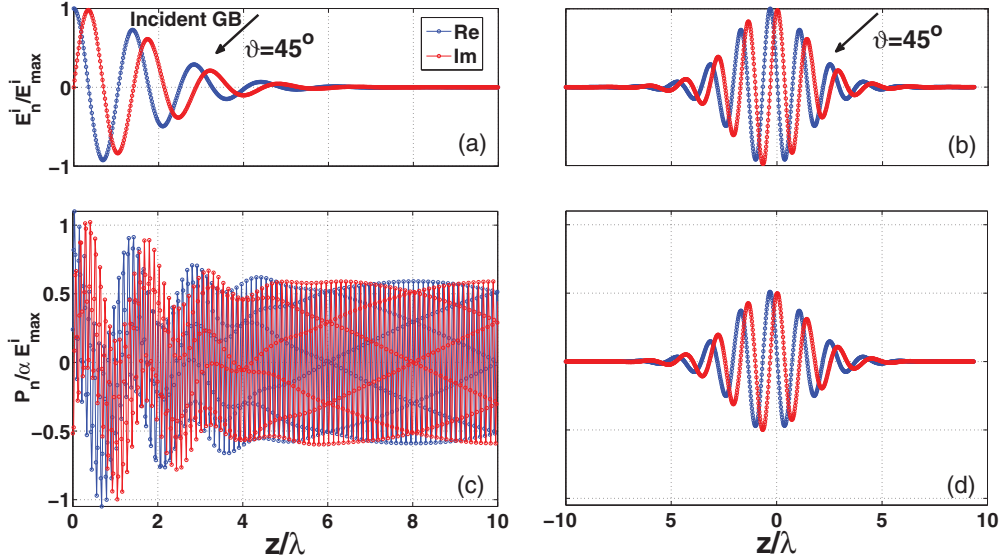


FIG. 11. (Color online) Chain excitation by a Gaussian beam. (a) E_n^i for a semi-infinite chain, hitting the chain end. (b) E_n^i for an infinite chain. (c) Response p_n of a semi-infinite chain. (d) p_n for infinite chain.

Green's function wave constituents can be discerned directly from the analytic properties of the chain's spectra in the complex Z plane. Each singularity represents a distinct wave phenomenon, the excitation strength of which is nothing but the associated residue; poles on the unit circle are guided modes, poles on trajectories off the unit circle are radiation modes, and branch cut constitutes the continuous spectrum. Due to this analytical clarity and physical transparency, a wave constituent in particle chains, the continuous spectrum wave, has been exposed. It is shown that this wave may dominate the chain response under lossy conditions. Physical insight on the various wave contributors in the infinite chain case is provided and contrasted with previous studies. By using a special extension of the Wiener-Hopf technique to the complex Z plane, our theory is then applied also to semi-infinite chains, and the edge effects are studied analytically. Special effort is placed toward expressing the semi-infinite Green's function in terms of the wave constituents associated with the corresponding infinite chain. The result provides physical insight on the edge effect: how the various wave constituents are reflected and/or intercoupled at the chain end. It is shown that the edge can significantly enhance chain excitation by external beams.

ACKNOWLEDGMENTS

This research was supported by the Israel Science Foundation (Grant No. 1503/10).

APPENDIX A: PROPERTIES OF Li_s

The series in Eq. (13) is strictly convergent only for $|z| \leq 1$. Analytic continuation of $Li_s(z)$ into the complex z plane is made possible by the integral relation

$$Li_{s+1}(z) = \int_0^z x^{-1} Li_s(x) dx, \quad (A1)$$

hence, $Li_s(z)$ inherits the singularity of $\ln(1-z) \forall s \geq 1$, possessing Riemann sheets of infinite multiplicity. Using the principal branch of the complex logarithm $-\pi < \Im(\ln z) \leq \pi$, it follows that, in the 0-Riemann sheet ($R0$), it has a branch point at $z = 1$, extending along the real positive z axis to $+\infty$, such that the axis is placed just below the cut.

The following properties are proved in Ref. 21. The discontinuity across the cut is given by $Li_s(z + i0^+) - Li_s(z) = 2\pi i [\ln(z)]^{s-1} / \Gamma(s)$, with z real and $z > 1$. Denote the value of $Li_s(z)$ at the n th Riemann sheet by $Li_s^{(Rn)}(z)$. Then,

$$Li_s^{(Rn)}(z) = Li_s^{(R0)}(z) - 2\pi i \frac{(\ln z)^{s-1}}{\Gamma(s)} n, \quad (A2)$$

where n counts the Riemann sheets in a counterclockwise direction. In the above, $\ln z$ possesses the regular branch-cut definition, hence, it increases by $2\pi i$ whenever the negative real z axis is crossed in a counterclockwise direction. It follows that on any Riemann sheet except for $R0$, $Li_s(z)$ possesses additional branch cut, emerging from the origin and extending along the negative z axes in the same fashion as the $\ln z$ cut. Finally, we note that, while the integral relation (A1) holds formally for any z , it may become inconvenient for large z . However, if $Li_s(z)$ is known for z inside the unit disk ($|z| \leq 1$), its analytic continuation to $|z| > 1$ can be computed via

$$Li_s(z) = (-1)^{s+1} Li_s\left(\frac{1}{z}\right) - \frac{1}{s!} [\ln(-z)]^s + 2 \sum_{r=1}^{\lfloor s/2 \rfloor} \frac{[\ln(-z)]^{s-2r}}{(s-2r)!} Li_{2r}(-1). \quad (A3)$$

APPENDIX B: ASYMPTOTIC BRANCH-CUT CONTRIBUTION

We derive here Eq. (21) describing the asymptotic (large- n) behavior of the continuous spectrum wave. The derivation shall be given for $n > 0$ and, therefore, we consider only

integration around the internal cut. By symmetry, the final result may be extended to any n by replacing n with $|n|$. We define a coordinate q along the cut by $Z = |q|e^{ikd}$. As Z changes along C_b in a counterclockwise direction, q roams over the interval $[-1, 1]$. The branch-cut contribution is given by Eq. (18). Consider the integrand $Z^{n-1}/\bar{D}(Z)$. For $n \gg 1$, we observe that along the cut, the integrand numerator is vanishingly small except for small regions near the branch point, corresponding to $q = \pm 1$. Consequently, for $n \gg 1$, we may replace the denominator of the integrand by an appropriate approximation, valid for $|q| \approx 1$,

$$\bar{D}(q) \approx \frac{k^2}{4\pi d\epsilon_0} [C - \ln(1 - |q|) - \pi i \operatorname{sgn}(q)] \quad (\text{B1})$$

with

$$\begin{aligned} C &= -\frac{kd}{\alpha} + L_{i_1}(e^{2ikd}) + \frac{i}{kd} \left(L_{i_2}(e^{2ikd}) + \frac{\pi^2}{6} \right) \\ &\quad - \frac{1}{(kd)^2} [L_{i_3}(e^{2ikd}) + \zeta(3)], \end{aligned} \quad (\text{B2})$$

where $\zeta(3) = 1.202 057$ is the Riemann zeta function of 3. In the derivation of Eq. (B1), we have used Eq. (A2) together with the fact that, for $|q| \approx 1$, $\ln(1 - |q|^{-1}) \approx \ln(1 - |q|) - \pi i$.

In order to demonstrate the validity of the arguments above, the original integrand and its approximation are shown in Fig. 12. It may be seen that as n increases, the approximation becomes more and more accurate. In addition, we observe that the integrand vanishes at the branch point. Hence, standard asymptotic techniques used in wave theory can not be applied. We use Eq. (B1) and rewrite Eq. (18) as

$$G_n^{(b)} \simeq \frac{4\pi\epsilon_0 d}{k^2} e^{inkd} \int_0^1 \frac{q^{n-1} dq}{\prod_{m=1}^n [\ln(1 - q) - A_m]} \quad (\text{B3})$$

with $A_{1,2} = C \pm \pi i$. By applying a second change of variable $u = -\ln(1 - q)$, we obtain

$$\begin{aligned} G_n^{(b)} &\simeq \frac{4\pi\epsilon_0 d}{k^2} e^{inkd} \\ &\quad \times \int_0^\infty \frac{(1 - e^{-u})^{n-1} e^{-u} du}{(u + A_1)(u + A_2)}. \end{aligned} \quad (\text{B4})$$

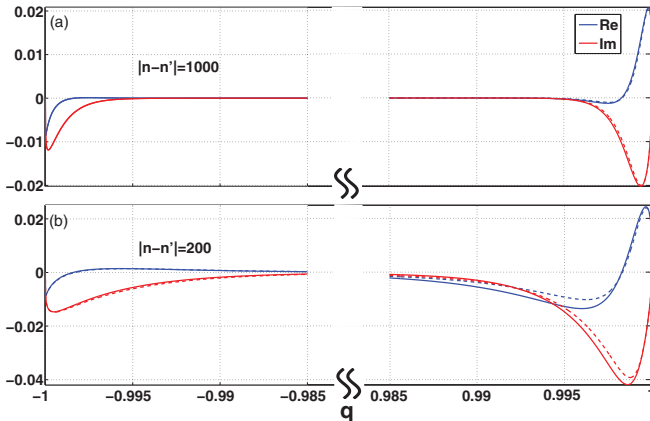


FIG. 12. (Color online) The integrand of Eq. (18) along the branch cut (solid lines) and its approximation (dashed lines). (a) for $|n - n'| = 1000$, $q < 0$ (just below the cut), $q > 0$ (just above the cut). (b) The same as (a) but for $|n - n'| = 200$.

Consider the integrand in Eq. (B4). The numerator is positive and very small almost on the entire $u > 0$ axis except for a region around its single maximum at $u_{\max} = \ln n$. Also, the denominator never vanishes, and changes rather slowly especially as u increases (the relevant domain of u for large n). Therefore, for large n , we use zeroth-order Taylor approximation in the vicinity of u_{\max} :

$$\frac{1}{u + A_{1,2}} \simeq \frac{1}{\ln n + A_{1,2}}. \quad (\text{B5})$$

We have validated that the higher-order terms do not contribute to the first asymptotic term in the final result. Finally, by using Eq. (B5) in Eq. (B4) and evaluating the resulting integral, we obtain Eq. (21).

APPENDIX C: PROOF OF IDENTITIES (28)–(31)

We prove the identities in Eqs. (28)–(31). An obvious identity is

$$\oint_{C_1} \frac{\ln \bar{D}(\zeta)}{Z - \zeta} d\zeta = \oint_{C_1} \frac{\ln D^+(\zeta)}{Z - \zeta} d\zeta + \oint_{C_1} \frac{\ln D^-(\zeta)}{Z - \zeta} d\zeta. \quad (\text{C1})$$

We start with $|Z| > 1$. In this case, the second term of the right-hand side vanishes (apply the residue theorem and recall that D^- is analytic and has no zeros inside the unit circle). The first term in the right-hand side can be evaluated by using the integration contour $C_1 \cup C_\infty$ shown in Fig. 13. Since $\ln D^+(\zeta)$ does not possess any singularity in the region enclosed (D^+ there is analytic and has no zeros there), we have

$$\int_{C_1 \cup C_\infty} \frac{\ln D^+(\zeta)}{Z - \zeta} d\zeta = 2\pi i \ln D^+(Z). \quad (\text{C2})$$

Hence, returning back to Eq. (C1),

$$\oint_{C_1} \frac{\ln \bar{D}(\zeta)}{Z - \zeta} d\zeta = 2\pi i \ln D^+(Z) - \oint_{C_\infty} \frac{\ln D^+(\zeta)}{Z - \zeta} d\zeta. \quad (\text{C3})$$

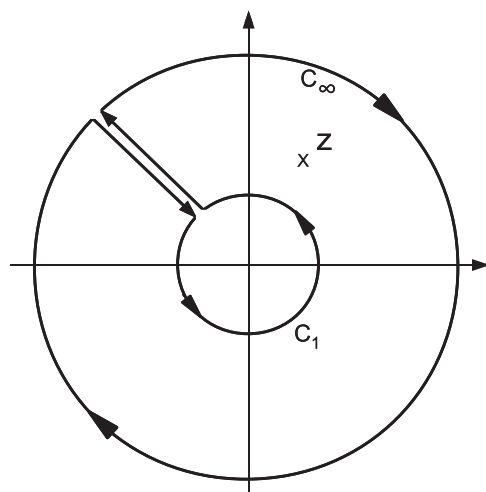


FIG. 13. Integration contours in the ζ plan.

With Eq. (27), we may replace $D^+(\zeta)$ in the integrand above by $D^-(0)$, so the surviving integral is a simple pole. We are left with

$$\oint_{C_1} \frac{\ln \bar{D}(\zeta)}{Z - \zeta} d\zeta = 2\pi i \ln D^+(Z) - 2\pi i \ln D^-(0). \quad (\text{C4})$$

By rearranging and exponentiating, we get

$$D^+(Z) = D^-(0) \exp \frac{1}{2\pi i} \oint_{C_1} \frac{\ln \bar{D}(\zeta)}{Z - \zeta} d\zeta. \quad (\text{C5})$$

By repeating the same procedure for $|Z| < 1$ and exploiting the analyticity of D^- inside C_1 and of D^+ between C_1 and C_∞ , we obtain

$$D^-(Z) = \frac{1}{D^-(0)} \exp \frac{-1}{2\pi i} \oint_{C_1} \frac{\ln \bar{D}(\zeta)}{Z - \zeta} d\zeta. \quad (\text{C6})$$

By setting $Z = 0$ in the equation above and defining $\lambda_0^{-1} = D^-(0)$, we obtain Eqs. (30) and (31). Using the definition of λ_0 in Eq. (C5), we obtain Eq. (28). The latter is valid only for $|Z| > 1$ and the expression itself is discontinuous when the pole at $\zeta = Z$ crosses the closed integration contour C_1 (at $|Z| = 1$). Inside the unit circle, $\ln \bar{D}(\zeta)$ has at most three branch cuts and no poles. One branch cut is due to \bar{D} itself (see Fig. 2), and two are due to the zeros of \bar{D} . Then, by using Cauchy theorem, we may replace C_1 by three integration paths along the cuts in a counterclockwise direction. Hence, for $|Z| > 1$, Eq. (28) is equivalent to

$$D^+(Z) = \frac{1}{\lambda_0} \exp \frac{1}{2\pi i} \oint_{\cup C_{bc}} \frac{\ln \bar{D}(\zeta)}{Z - \zeta} d\zeta. \quad (\text{C7})$$

With this expression, $D^+(Z)$ changes continuously when Z is continued into the unit circle, so it may be

considered as the analytic continuation. If we now set $|Z| < 1$, a single pole is introduced inside the unit circle. The passage from the contours $\cup C_{bc}$ to the more convenient contour C_1 should take this pole into account via its residue. Hence, using C_1 , we have for $|Z| < 1$ the result that gives Eq. (29):

$$D^+(Z) = \frac{1}{\lambda_0} \exp \frac{1}{2\pi i} \oint_{C_1} \frac{\ln[\bar{D}(\zeta)/\bar{D}(Z)]}{Z - \zeta} d\zeta. \quad (\text{C8})$$

APPENDIX D: PROOF OF EQ. (37)

We multiply Eq. (36) by $Z^{j'-1}$, integrate along C_1 , use $E^+(Z) = Z^{-n'}$ and Eq. (33), and apply Cauchy's theorem. The result is

$$a_j = \frac{1}{2\pi i} \oint_{C_1} \frac{Z^{j-n'-1}}{D^-(Z)} dZ - \frac{1}{2\pi i} \oint_{C_1} \left(\frac{E^+}{D^-} \right)^- (Z) Z^{j-1} dZ, \quad (\text{D1})$$

where we changed $j' \rightarrow j$. The second integrand on the right is analytic inside the unit circle for $j \geq 1$. Recall that $\bar{E}^-(Z) = \sum_{n=-\infty}^{-1} E_n^- Z^{-n} \Rightarrow \bar{E}^-(0) = 0$. Since the right-hand side of Eq. (34) vanishes (see the preceding discussion), it follows that $(\bar{E}^+/D^-)^-$ vanishes too for $Z = 0$ (D^- is analytic and has no zeros inside the unit circle). Hence, in the second integrand above, analyticity in the unit circle and at the origin is maintained also for $j = 0$. Consequently, by Cauchy's theorem, the second integral vanishes for $j \geq 0$. Regarding the first integral, by the properties of D^- mentioned above, the integrand is analytic for $j \geq n' + 1$. This yields Eq. (37).

*hadady@eng.tau.ac.il

[†]Corresponding author: steinber@eng.tau.ac.il

¹M. Quinten, A. Leitner, J. R. Krenn, and F. R. Aussenegg, *Opt. Lett.* **23**, 1331 (1998).

²S. A. Tretyakov and A. J. Viitanen, *Electr. Eng. (Am. Inst. Electr. Eng.)* **82**, 353 (2000).

³M. L. Brongersma, J. L. Hartman, and H. A. Atwater, *Phys. Rev. B* **62**, R16356 (2000).

⁴W. H. Weber and G. W. Ford, *Phys. Rev. B* **70**, 125429 (2004).

⁵A. F. Koenderink and A. Polman, *Phys. Rev. B* **74**, 033402 (2006).

⁶T. Yang and K. B. Crozier, *Opt. Express* **16**, 8570 (2008).

⁷Andrea Alu and Nader Engheta, *Phys. Rev. B* **74**, 205436 (2006).

⁸D. V. Orden, Y. Fainman, and V. Lomakin, *Opt. Lett.* **34**, 422 (2009).

⁹D. V. Orden, Y. Fainman, and V. Lomakin, *Opt. Lett.* **35**, 2579 (2010).

¹⁰Y. Hadad and Ben Z. Steinberg, *Phys. Rev. Lett.* **105**, 233904 (2010).

¹¹Saber N. Elaydi, *An Introduction to Difference Equations*, 3rd ed. (Springer, New York, 2005).

¹²Eliahu I. Jury, *Theory and Application of the Z-Transform Method* (Wiley, New York, 1964).

¹³W. Wasylkiwskyj, *IEEE Trans. Antennas Propag.* **21**, 277 (1973).

¹⁴C. M. Linton and P. A. Martin, *SIAM J. Appl. Math.* **64**, 1035 (2004).

¹⁵F. Capolino and M. Albani, *Radio Sci.* **44**, RS2S91 (2009).

¹⁶V. A. Markel and A. K. Sarychev, *Phys. Rev. B* **75**, 085426 (2007).

¹⁷A. G. Govyadinov and V. A. Markel, *Phys. Rev. B* **78**, 035403 (2008).

¹⁸D. S. Citrin, *Nano Lett.* **5**, 985 (2005).

¹⁹D. S. Citrin, Y. Wang, and Z. Zhou, *J. Opt. Soc. Am. B* **25**, 937 (2008).

²⁰S. A. Maier, P. G. Kik, and H. A. Atwater, *Phys. Rev. B* **67**, 205402 (2003).

²¹Leonard Lewin, *Polylogarithms and Associated Functions* (Elsevier, New York, 1981).

²²F. Olyslager, *Electromagnetic Waveguides and Transmissin Lines* (Clarendon, Oxford, 1999).